TEN-VERTEX POLYHEDRAL MONOCARBABORANE CHEMISTRY. THE NOVEL HIGH-YIELD FORMATION OF THE TEN-VERTEX *closo* COMPOUND [6-(PMe_2Ph)-*closo*-1-CB_9H_9] FROM THE THERMOLYSIS OF [8,8-$(PMe_2Ph)_2$-*nido*-8,7-$PtCB_9H_{11}$]*

Jane H. JONES[a], Bohumil ŠTÍBR[b], John D. KENNEDY[a] and Mark THORNTON-PETT[a]

[a] *School of Chemistry,*
University of Leeds, Leeds LS2 9JT, England
[b] *Institute of Inorganic Chemistry,*
Academy of Sciences of the Czech Republic, 25068 Řež u Prahy, The Czech Republic

Received November 2, 1992
Accepted December 7, 1992

Thermolysis of [8,8-$(PMe_2Ph)_2$-*nido*-8,7-$PtCB_9H_{11}$] in boiling toluene solution results in an elimination of the platinum centre and cluster closure to give the ten-vertex *closo* species [6-(PMe_2Ph)-*closo*-1-CB_9H_9] in 85% yield as a colourless air-stable solid. The product is characterized by NMR spectroscopy and single-crystal X-ray diffraction analysis. Crystals (from hexane–dichloromethane) are monoclinic, space group $P2_1/c$, with a = 903.20(9), b = 1 481.86(11), c = 2 320.0(2) pm, β = 97.860(7)° and Z = 8, and the structure has been refined to $R(R_w)$ = 0.045(0.051) for 3 281 observed reflections with $F_o > 2.0\sigma(F_o)$. The clean high-yield elimination of a metal centre from a polyhedral metallaborane or metallaheteroborane species is very rare.

The thermolysis of *closo* metallaboranes and metallaheteroboranes generally results in cluster isomerisation if it does not result in a general decomposition[1,2]. Thermolysis of the more open *nido* and *arachno* species if not resulting in general decomposition generally results in dihydrogen loss[1,2], accompanied by cluster closure or by other condensation processes such as cycloboronation of P-phenyl groups on phosphine ligands that may be attached to the metal[3]. These condensations may be accompanied by a variety of other processes such as cluster-vertex loss, and such cluster degradations are often encouraged if nucleophiles are present. In reported work, in only one instance does thermolysis result in substantial cluster agglommeration, this being in the "aufbau" thermolysis of [4,4-$(PMe_2Ph)_2$-*arachno*-4-PtB_8H_{12}] to form macropolyhedral platinaboranes of fourteen vertices and more[4]. All these thermolytic processes, however, are characterized by a retention of the metal-to-borane or metal-to-heteroborane linkages.

---

* Contribution No. 30 from the Řež-Leeds Anglo-Czech Polyhedral Collaboration (A.C.P.C.).

The identified major products in all reactions reported so far have always been polyhedral metallaborane or metallaheteroborane species, the one possible exception to this being the PMe_2Ph-induced cluster comproportionation of eleven-vertex [7,7-$(PMe_2Ph)_2$-*nido*-7-$PtB_{10}H_{12}$] to give various isomers and derivatives of *closo*-type twelve-vertex diplatinaboranes such as [1,1,2,2-$(PMe_2Ph)_4$-*closo*-1,2-$Pt_2B_{10}H_{10}$] and of the *closo* ten-vertex non-metallated species [$(PMe_2Ph)_2$-*closo*-$B_{10}H_8$] (ref.[5]).

We now report here the first example of a clean high-yield elimination of the metal vertex from a metallaheteroborane or metallaborane cluster, viz. in the thermolysis of eleven-vertex [8,8-$(PMe_2Ph)_2$-*nido*-8,7-$PtCB_9H_{11}$] in boiling toluene solution to give the ten-vertex *closo* species [6-(PMe_2Ph)-*closo*-1-CB_9H_9] in 85% yield. The work forms part of a general survey of the synthesis, structure, and behaviour of polyhedral metallaheteroboranes incorporating the {$Pt(PMe_2Ph)_2$} unit as a standard metal centre (for other recent work see refs[6 – 8]).

RESULTS AND DISCUSSION

Straightforwardly heating a solution of [8,8-$(PMe_2Ph)_2$-*nido*-8,7-$PtCB_9H_{11}$] (ref.[8]) in boiling toluene, followed by chromatographic separation of the reaction products, resulted in the isolation of a colourless crystalline solid, identified as [6-(PMe_2Ph)-*closo*-1-CB_9H_9], in 85% yield (reaction scale 50 μmol). As mentioned in the introduction, this is a rather unusual process, and in this context the high yield is noteworthy.

$$[8,8\text{-}(PMe_2Ph)_2\text{-}nido\text{-}8,7\text{-}PtCB_9H_{11}] \longrightarrow$$

$$[6\text{-}(PMe_2Ph)\text{-}closo\text{-}1\text{-}CB_9H_9] + \{3\ PMe_2Ph + Pt + H_2\} \qquad (A)$$

It will be of obvious interest to determine the fate of the {$3PMe_2Ph + Pt + H_2$} in this unusual process, and we are currently devising experiments with this in mind.

Crystals suitable for X-ray diffraction analysis were grown by causing hexane to slowly diffuse into a dichloromethane solution of the complex. The diffraction data set was collected at 200 K (see Experimental) enabling the ready location of all cluster hydrogen atoms. Final atomic co-ordinates and equivalent isotropic thermal parameters are given in Table I and the molecular structure of one of the molecules (see below) and its numbering scheme is shown in Fig. 1. Selected interatomic distances and angles are given in Tables II and III, respectively. The compound is readily seen to have a *closo* ten-vertex cluster structure based on a bicapped square antiprism. There is a carbon atom in the "polar" (1-) position of low connectivity as in the previously determined[9] anion $[CB_9H_{10}]^-$. However, in this instance, there is a dimethylphenylphosphine substituent attached to the 6-position and the complex is neutral. The overall *closo* nature is in complete accord with the Williams–Wade cluster-geometry[10] and electron-counting[11] formalism.

TABLE I

Non-hydrogen and cluster-hydrogen fractional atomic co-ordinates (. 10^4) for [6-(PMe_2Ph)-*closo*-1-CB_9H_9] with estimated standard deviations (e.s.d.'s) in parentheses

Atom	x	y	z	$U_{iso}/U_{eq}{}^a$
		Molecule 1		
P(1)	4510.2(7)	6936.8(4)	1125.8(3)	30.4(2)
C(11)	5268(3)	7486(2)	544(1)	44(1)
C(12)	5081(3)	7559(2)	1783(1)	46(1)
C(131)	5344(2)	5833(1)	1219(1)	33(1)
C(132)	5905(2)	5405(1)	759(1)	48(1)
C(133)	6582(2)	4560(1)	843(1)	65(1)
C(134)	6699(2)	4144(1)	1387(1)	67(1)
C(135)	6138(2)	4573(1)	1847(1)	73(1)
C(136)	5461(2)	5417(1)	1763(1)	55(1)
C(1)	35(3)	5803(2)	1101(1)	46(1)
B(2)	1340(3)	6363(2)	1482(1)	39(1)
B(3)	1417(4)	5894(2)	743(1)	41(1)
B(4)	-469(4)	6333(3)	507(1)	43(1)
B(5)	-541(4)	6791(3)	1234(1)	45(1)
B(6)	2388(3)	6915(2)	980(1)	31(1)
B(7)	1138(3)	6888(2)	293(1)	39(1)
B(8)	-252(3)	7528(2)	637(2)	44(1)
B(9)	1035(3)	7549(2)	1329(1)	42(1)
B(10)	1561(4)	7859(2)	676(2)	42(1)
H(1)	-310(37)	5213(25)	1238(15)	42(1)
H(2)	1780(30)	6133(19)	1919(13)	81(1)
H(3)	2017(27)	5277(18)	608(11)	56(1)
H(4)	-1321(34)	6070(19)	183(13)	42(1)
H(5)	-1482(29)	6894(17)	1502(12)	62(1)
H(7)	1342(27)	6834(15)	-160(11)	40(1)
H(8)	-1268(29)	8022(17)	428(11)	48(1)
H(9)	1284(26)	8049(16)	1767(10)	32(1)
H(10)	2001(31)	8535(19)	528(12)	53(1)

TABLE I
(*Continued*)

Atom	x	y	z	U_{iso}/U_{eq} [a]
		Molecule 2		
P(1)	322.4(7)	5857.6(4)	3590.3(3)	33.6(3)
C(11)	−265(4)	5434(2)	4247(2)	59(1)
C(12)	−475(3)	5146(2)	3003(2)	63(1)
C(131)	−475(3)	6957(1)	3447(1)	31(1)
C(132)	−611(2)	7306(1)	2883(1)	45(1)
C(133)	−1239(2)	8157(1)	2764(1)	53(1)
C(134)	−1738(2)	8659(1)	3208(1)	54(1)
C(135)	−1609(2)	8311(1)	3771(1)	56(1)
C(136)	−980(2)	7460(1)	3891(1)	41(1)
C(1)	4860(3)	6926(2)	3703(1)	41(1)
B(2)	3528(3)	6681(2)	4057(1)	38(1)
B(3)	3474(3)	6561(2)	3260(1)	35(1)
B(4)	5327(3)	6044(2)	3382(1)	40(1)
B(5)	5378(4)	6158(2)	4168(1)	41(1)
B(6)	2441(3)	5815(2)	3661(1)	32(1)
B(7)	3689(2)	5355(2)	3183(1)	40(1)
B(8)	5037(3)	5077(2)	3825(2)	44(1)
B(9)	3758(4)	5529(2)	4304(1)	42(1)
B(10)	3201(4)	4772(2)	3763(2)	44(1)
H(1)	5349(33)	7516(23)	3672(13)	65(1)
H(2)	2992(26)	7207(17)	4314(10)	36(1)
H(3)	2994(31)	6963(20)	2911(13)	57(1)
H(4)	6220(31)	6089(17)	3103(12)	60(1)
H(5)	6314(29)	6278(17)	4515(11)	42(1)
H(7)	3473(26)	5038(17)	2728(10)	38(1)
H(8)	5999(32)	4522(20)	3852(12)	61(1)
H(9)	3456(29)	5356(18)	4787(12)	54(1)
H(10)	2572(27)	4083(16)	3739(10)	35(10)

[a] U_{eq} is defined as one third of the trace of the orthogonalised U_{ij} tensor.

The complex crystallizes with two symmetry-independent molecules in the asymmetric part of the unit cell. The two molecules differ (i) by a slight rotation of the phosphine ligand relative to the carbaborane cage so that, for instance, B(10)–B(6)–P(1)–C(12) is 79.6(2)° for molecule 1 and 60.9(2)° for molecule 2, and (ii) by a slight rotation of the phenyl ring of the phosphine ligand relative to the two methyl substituents so that, for instance, C(132)–C(131)–P(1)–C(11) is 24.8(2)° for molecule 1 and 20.7(2)° for molecule 2. There are, however, no significant differences between equivalent bond distances and angles (see Tables II and III).

Distances between the polar carbon atom and the tropical boron atoms are significantly shorter than the tropical-polar boron-boron distances which in turn are shorter than the inter- and intratropical distances. This trend is mirrored[9,12] in $[CB_9H_{10}]^-$ and (where appropriate) $[B_{10}H_{10}]^{2-}$. There is a suggestion that distances between boron atoms of the same tropical belt [181.8(6) – 186.1(6) pm] may be slightly longer than those between connected atoms of different belts [179.6(6) – 181.6(6) pm]. The ranges are however very close, of course, so this difference may not be significant.

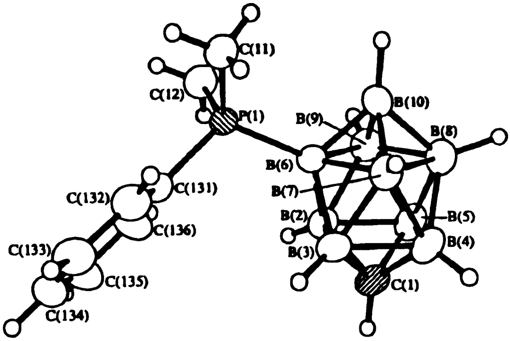

Molecule 1

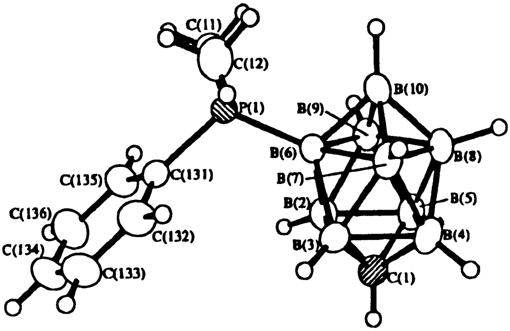

Molecule 2

FIG. 1

ORTEP-type diagram of the crystallographically determined molecular structure of [6-(PMe_2Ph)-*closo*-1-CB_9H_9]

At first sight the phosphine substituent does not exhibit any major steric or electronic influence on the geometry of the carbaborane cage which, in both molecules, approximates very closely to the ideal[10] C_{4v}/D_{4d} *closo* ten-vertex symmetry. However it has recently been noted that ten-vertex formally *closo* heteroborane clusters invariably posses a more open or "stretched" intratropical bond between two boron atoms adjacent to the heteroatom[9,13]. This opening varies markedly among known compounds, and their structures consequently exhibit a continuum of behaviour[13], of which one of the variable parameters is this interboron distance. This separation ranges from 192 pm (ref.[13]) for *closo*-$[CB_9H_{10}]^-$ to values of 230 pm for so-called *isonido* complexes such as $[(PPh_3)(Ph_2PC_6H_4)ClIrB_9H_5(OEt)(PPh_3)]$[9,14]. When the heteroatom is not a transition element strong contributions to this effect derive from the asymmetrization of cluster electron density that arises from the heteroatom of the cluster[7]. In this general context it is interesting to note that in the $[6\text{-}(PMe_2Ph)\text{-}$*closo*$\text{-}1\text{-}CB_9H_9]$ species there is one intratropical distance, B(2)–B(3) in Fig. 1, which averages at 185.6(6) pm and which is

TABLE II

Selected interatomic distances (pm) for $[6\text{-}(PMe_2Ph)\text{-}$*closo*$\text{-}1\text{-}CB_9H_9]$, with e.s.d.'s in parentheses

Atoms	Distance		Atoms	Distance	
	molecule 1	molecule 2		molecule 1	molecule2
C(11)–P(1)	179.1(4)	179.4(5)	C(131)–P(1)	180.1(3)	179.7(3)
C(12)–P(1)	179.6(5)	179.4(5)	B(6)–P(1)	190.1(5)	190.0(5)
B(2)–C(1)	160.5(6)	158.9(6)	B(3)–C(1)	159.6(6)	160.1(6)
B(4)–C(1)	159.6(6)	158.9(6)	B(5)–C(1)	159.8(7)	159.5(6)
B(3)–B(2)	186.1(6)	185.1(6)	B(5)–B(4)	182.8(6)	182.6(6)
B(5)–B(2)	183.0(6)	182.8(6)	B(4)–B(3)	183.5(7)	182.8(6)
B(6)–B(2)	179.6(6)	179.1(6)	B(6)–B(3)	179.8(6)	178.7(6)
B(9)–B(2)	180.6(7)	180.4(6)	B(7)–B(3)	180.4(6)	181.0(6)
B(7)–B(4)	179.6(6)	180.5(6)	B(9)–B(5)	180.3(6)	179.9(6)
B(8)–B(4)	180.4(7)	180.3(7)	B(8)–B(5)	181.1(7)	179.6(7)
B(7)–B(6)	182.4(6)	181.8(6)	B(9)–B(6)	181.6(6)	182.6(6)
B(10)–B(6)	169.4(6)	169.4(6)	B(10)–B(8)	170.0(6)	170.6(6)
B(8)–B(7)	184.1(6)	183.7(7)	B(9)–B(8)	184.9(7)	183.6(6)
B(10)–B(7)	170.7(7)	170.6(7)	B(10)–B(9)	171.3(6)	170.8(7)
H(1)–C(1)	99(4)	99(3)	H(2)–B(2)	109(3)	113(3)
H(3)–B(3)	113(3)	105(3)	H(4)–B(4)	107(3)	110(3)
H(5)–B(5)	113(3)	110(3)	H(7)–B(7)	109(3)	115(3)
H(8)–B(8)	122(3)	119(3)	H(9)–B(9)	125(2)	122(3)
H(10)–B(10)	115(3)	117(3)			

slightly longer than the others, although still significantly outside the range of 192 – 230 pm quoted above. This is the linkage flanked by the C(1)H and the B(6)(PMe$_2$Ph) centres which suggests that the asymmetrization induced by the carbon atom (as in the [CB$_9$H$_{10}$]$^-$ anion) is compensated by the effect of the phosphine substituent on B(6). It will be of interest to see rigorous quantum-chemical calculations associated with these phenomena.

Since NMR parameters are intimately dependent upon electronic structure it was of interest to compare the assigned ^{11}B and ^{1}H spectra of [6-(PMe$_2$Ph)-*closo*-1-CB$_9$H$_9$] with its formally isoelectronic congeners [B$_{10}$H$_{10}$]$^{2-}$, [1,6-(PMe$_2$Ph)$_2$B$_{10}$H$_8$], [1-CB$_9$H$_{10}$]$^-$ and [1,6-C$_2$B$_8$H$_{10}$] to assess the affects of interchange of the mutually isolobal units {BH}$^-$, {CH}, and {B(PMe$_2$Ph)} among the 1- and 6-sites and thereby ultimately to examine for similarity of electronic structure. Table IV gives the measured NMR data

TABLE III
Selected angles (°) between interatomic vectors for [6-(PMe$_2$Ph)-*closo*-1-CB$_9$H$_9$] with e.s.d.'s in parentheses

Atoms	Angle		Atoms	Angle	
	molecule 1	molecule 2		molecule 1	molecule 2
C(131)-P(1)-C(11)	107.8(2)	108.4(2)	C(131)-P(1)-C(12)	107.3(2)	106.4(2)
C(12)-P(1)-C(11)	108.1(2)	107.7(3)	B(6)-P(1)-C(13)	113.7(2)	115.0(2)
B(6)-P(1)-C(11)	110.7(2)	109.0(2)	B(6)-P(1)-C(12)	109.9(2)	109.9(2)
B(3)-C(1)-B(2)	71.1(3)	70.9(3)	B(5)-C(1)-B(4)	69.8(3)	70.0(3)
B(4)-C(1)-B(2)	108.8(3)	108.8(3)	B(5)-C(1)-B(3)	108.8(3)	108.9(3)
B(4)-C(1)-B(3)	70.2(3)	69.9(3)	B(5)-C(1)-B(2)	69.7(3)	70.1(3)
B(3)-B(2)-C(1)	54.2(3)	54.8(3)	B(2)-B(3)-C(1)	54.7(3)	54.2(3)
B(5)-B(2)-C(1)	55.0(3)	55.1(3)	B(4)-B(3)-C(1)	54.9(3)	54.7(3)
B(6)-B(2)-C(1)	106.9(3)	107.4(3)	B(6)-B(3)-C(1)	107.2(3)	107.0(3)
B(5)-B(2)-B(3)	89.4(3)	90.0(3)	B(4)-B(3)-B(2)	89.6(3)	89.2(3)
B(6)-B(2)-B(3)	58.9(3)	58.8(3)	B(6)-B(3)-B(2)	58.8(3)	58.9(3)
B(9)-B(2)-B(3)	101.9(3)	102.3(3)	B(7)-B(3)-B(2)	102.0(3)	101.8(3)
B(2)-B(6)-P(1)	120.0(3)	119.7(3)	B(3)-B(6)-P(1)	120.4(3)	121.7(3)
B(7)-B(6)-P(1)	130.1(2)	131.4(2)	B(9)-B(6)-P(1)	129.4(3)	127.9(3)
B(10)-B(6)-P(1)	115.9(3)	115.3(3)	B(3)-B(6)-B(2)	62.4(3)	62.3(3)
B(10)-B(6)-B(2)	113.9(3)	113.5(3)	B(10)-B(6)-B(3)	113.5(3)	114.0(3)
B(7)-B(6)-B(2)	103.8(3)	103.8(3)	B(9)-B(6)-B(2)	60.0(3)	59.8(3)
B(7)-B(10)-B(6)	64.8(3)	64.7(3)	B(9)-B(10)-B(6)	64.4(3)	64.9(3)
B(8)-B(10)-B(6)	98.6(3)	98.1(3)	B(9)-B(10)-B(7)	99.5(3)	99.5(3)
B(8)-B(10)-B(7)	65.4(3)	65.1(3)	B(9)-B(10)-B(8)	65.6(3)	65.1(3)

for [6-(PMe_2Ph)-*closo*-1-CB_9H_9], with data, some previously unreported in the literature, for the other four compounds summarized in Table V.

Figure 2 (lower diagrams) compares the chemical shifts and relative intensities in the ^{11}B NMR spectra of these five species. It can be seen that the basic shielding patterns are all very similar, with the ^{11}B NMR signals from the tropical positions being closely grouped in the region $\delta(^{11}B)$ −20 to −30 ppm, and with the signals from the axial positions appearing at somewhat lower fields. The similarity confirms the expected close parallels in the electronic structure. Within this context, however, it is apparent that there is a marked antipodal deshielding effect at the B(10) position in the closed ten-vertex cluster when $\{BH(1)\}^-$ in $[B_{10}H_{10}]^{2-}$ is replaced by {CH} or $\{B(PMe_2Ph)\}$. It is most marked for the {CH} replacement, which induces a shift of 20 to 30 ppm to low field. The replacement of $\{BH\}^-$ by $\{B(PMe_2Ph)\}$ has a smaller, but still very significant, effect of ca 12 ppm. In contrast to this axial–axial trans-cluster antipodal effect, which has in fact been well documented[17] and discussed[18,19] with respect to carbon and other cluster heterosubstituents (although we believe that this is the first instance of it being documented for a {B(ligand)} residue), it is interesting that there is

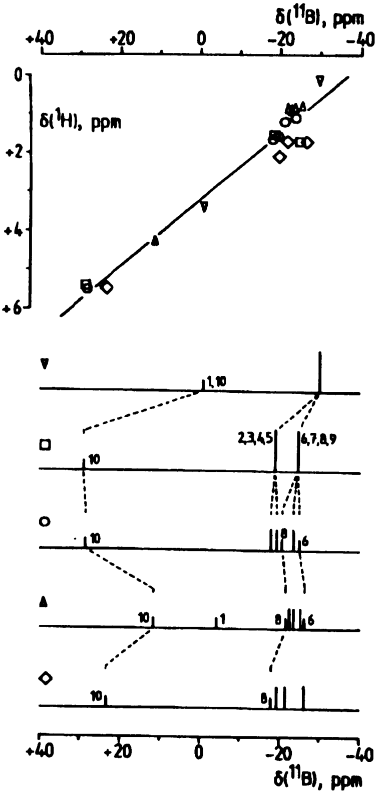

FIG. 2

NMR data for [6-(PMe_2Ph)-*closo*-1-CB_9H_9] (○, this work), together with those for [*closo*-$B_{10}H_{10}$]$^{2-}$ (▽, ref.[15]), [*closo*-1-CB_9H_{10}]$^-$ (□, ref.[9]), [1,6-$(PMe_2Ph)_2$-*closo*-$B_{10}H_8$] (Δ, ref.[16]), and [*closo*-1,6-$C_2B_8H_{10}$] (◊, this work) for comparison. The top diagram is a plot of $\delta(^1H)$ vs $\delta(^{11}B)$ for individual BH(*exo*) units, and the line drawn has slope $\delta(^1H)$: $\delta(^{11}B)$ of 1 : 11.5, intercept +3.2 in $\delta(^1H)$. The bottom diagrams are stick representations of the chemical shifts and relative intensities in the ^{11}B spectra, with hatched lines connecting equivalent positions in the compounds no significant tropical–tropical trans-cluster antipodal effect at B(8) arising from replacement of trans-cluster $\{BH(6)\}^-$ with $\{B(PMe_2Ph)\}$ or $\{CH\}$. A second interesting axial–axial antipodal phenomenon is the manifestation of a finite interproton coupling constant (formally $^5J(^1H-^1H)$ in the observed $[^1H-^1H]$-COSY correlation cross peak between the (1)- and (10)-proton resonances (footnote *c*, Table IV).

EXPERIMENTAL

General

NMR spectroscopy. Nuclear magnetic resonance spectroscopy was performed as detailed in other recent papers from our laboratories[20,21], with chemical shifts δ being given in ppm to high frequency (low field) of Ξ = 40.480730 MHz for ^{31}P (nominally 85% H_3PO_4), Ξ = 32.083971 MHz (nominally F_3BOEt_2 in $CDCl_3$) for ^{11}B (quoted ±0.5 ppm) and Ξ = 100 MHz for ^1H (quoted ±0.05 ppm), Ξ being defined as in ref.[22].

Thermolysis of [8,8-$(PMe_2Ph)_2$-nido-8,7-$PtCB_9H_{11}$]. The reaction was carried out under an inert atmosphere of dry nitrogen, although subsequent manipulations were carried out in air. Dried and degassed solvents were used throughout. [8,8-$(PMe_2Ph)_2$-*nido*-8,7-$PtCB_9H_{11}$] (30 mg; 51 μmol, prepared as in ref.[8]) was added to toluene (ca 20 cm^3). The pale yellow solution was then heated at reflux temperature for 3 h and then cooled. The resulting yellow solution was filtered through silica and the silica washed with toluene (ca 20 cm^3). The filtrate was then reduced to dryness (rotary evaporator; ca 323 K; water-pump pressure), redissolved in CH_2Cl_2 (ca 5 cm^3) and applied to a preparative TLC plate (silica G; Fluka type GF254). This was developed using CH_2Cl_2 as the liquid phase, yielding a pale yellow band (R_F ≈ 0.85) and a number of streaked areas. These were all removed from the silica (each with CH_2Cl_2; ca 30 cm^3). Repeated TLC work on the pale yellow band

TABLE IV
Measured NMR parameters for [6-(PMe_2Ph)-*closo*-1-CB_9H_9] in $CDCl_3$ at 294 – 297 K

Assigment	$\delta(^{11}B)$	Observed $[^{11}B-^{11}B]$-COSY correlations	$\delta(^1H)$	Observed $[^1H-^1H]$-COSY correlations[a]
10	28.5[b]	8 *m* 7,9 *w* 6 *w*	5.49	8 *m* 7,9 *s* 1 *w*
4,5	−17.8	2,3 *s* 8 *w* 7,9 *w*	1.66	8 *w* 7,9 *w* 1 *m*
2,3	−19.2	4,5 *s* 8 *s* 6 *m* 7,9 *w*	1.58	7,9 *m* 1 *s*
8	−20.7	10 *m* 4,5 *w* 2,3 *s*	1.17	10 *m* 4,5 *w*
7,9	−23.6	10 *w* 4,5 *w*	1.07	10 *s* 4,5 *w* 2,3 *m*
6	−24.8[c]	10 *w* 2,3 *m* 7,9 *m*	$[PMe_2Ph]$[d]	–
1	[CH]	–	5.14[e]	10 *w* 4,5 *m* 2,3 *s*

[a] Experiment carried out under conditions of complete $\{^{11}B$(broadband noise)$\}$ decoupling. Any $[^1H-^1H]$ correlations between $^1H(4,5)$ and $^1H(2,3)$, and between $^1H(8)$ and $^1H(7,9)$ not observable due to ^1H peak overlap. [b] $^1J(^{11}B-^1H)$ 158 Hz (other similar couplings obscured by peak overlap). [c] $\delta(^{31}P)$ −4.25 ppm; $^1J(^{31}P-^{11}B)$ 155 Hz. [d] $\delta(^1H)(PMe_2)$ +1.71, doublet, $^2J(^{31}P-^1H)$ 12.5 Hz. [e] Fine structure observed, with $^3J(^1H-^1H)$ and $^4J(^{31}P-^1H)$ all ca 3 – 4 Hz; note also the antipodal, formally $^5J(^1H-^1H)$, $[^1H-^1H]$-COSY correlation observed to $^1H(10)$.

TABLE V

NMR data for [*closo*-1-CB_9H_{10}]$^-$ (*a*), [*closo*-$B_{10}H_{10}$]$^{2-}$ (*b*), [1,6-(PMe_2Ph)$_2$-*closo*-$B_{10}H_8$] (*c*), and [*closo*-1,6-$C_2B_8H_{10}$] (*d*)

a) $[NMe_4]^+[CB_9H_{10}]^-$ in $CDCl_3$ at 294 – 297 K (data from ref.[9])

Assigment	$\delta(^{11}B)$	Observed [^{11}B-^{11}B]-COSY correlations	$\delta(^1H)$
10	28.9	6,7,8,9	5.44
2,3,4,5	−19.2	6,7,8,9	1.50
6,7,8,9	−24.7	10,2,3,4,5	1.70
1	[CH]	–	4.90

b) $[NHEt_3]^+_2\,[B_{10}H_{10}]^{2-}$ in D_2O at 294 K (data from ref.[15])

Assigment	$\delta(^{11}B)$	$\delta(^1H)$
1,10	−0.8	3.36
2 – 9	−29.9	0.10

c) $[1,6\text{-}(PMe_2Ph)_2B_{10}H_8]^a$ in CD_2Cl_2 at 294 K (data from ref.[16])

Assigment	$\delta(^{11}B)$	$\delta(^1H)$
1	−4.5[b,c]	–
2,3	−22.5	0.88
4,5	−23.6	0.83
7,9	−25.3	0.78
6	−26.1[c,d]	–
8	−21.9	0.85
10	11.7	4.27

d) $[1,6\text{-}C_2B_8H_{10}]$ in CD_2Cl_2 at 294 – 297 K (this work)

Assigment	$\delta(^{11}B)$	$\delta(^1H)$
1	[CH]	5.28
2,3	−19.3	2.09
4,5	−21.5	1.62
6	[CH]	1.96
7,9	−26.4	1.69
8	−17.8	1.65
10	23.4	5.47

[a] 1,10 isomer has $\delta(^{11}B)(1,10)$ +3.0 ($^1J(^{31}P\text{-}^{11}B)$ 195 Hz), $\delta(^{11}B)(2-9)$ −20.9, $\delta(^{31}P)$ −6.3. [b] Doublet structure from $^1J(^{31}P\text{-}^{11}B)$ 197 Hz. [c] Both $\delta(^{31}P)$ values very close at ca −7 ppm. [d] Doublet structure from $^1J(^{31}P\text{-}^{11}B)$ 180 ± 25 Hz.

thence yielded [6-(PMe$_2$Ph)-*closo*-1-CB$_9$H$_9$] (11 mg; 43 µmol; 85%) as the major product. 28 MHz ^{11}B NMR spectroscopy showed that other components did not contain any significant quantity of boron.

Single-Crystal X-Ray Diffraction Analysis

All measurements were carried out on a Stoe STADI4 diffractometer using an ω/θ scan mode and graphite-monochromated copper K_α radiation (λ = 154.184 pm). The data set was corrected for absorption using azimuthal psi scans. The structure was solved by direct methods using SHELXS86 (ref.[23]) and was refined by full-matrix least-squares (based on F) using SHELX76 (ref.[24]). All non-hydrogen atoms were refined with anisotropic thermal parameters, and the phenyl groups were treated as rigid bodies with idealized hexagonal symmetry (C–H = 139.5 pm). The phenyl and methyl hydrogen atoms were included in calculated positions (C–H = 95 pm) and were assigned to an overall isotropic thermal parameter. The cluster hydrogen atoms were located on a Fourier difference map and were freely refined with individual isotropic thermal parameters. The weighting scheme $w^{-1} = \sigma^2(F_o) + 0.0004\,(F_o)^2$ was used.

Crystal data. C$_9$H$_{20}$B$_9$P, M = 256.5, a = 903.20(9), b = 1 481.86(11), c = 2 320.0(2) pm, β = 97.860(7)°, U = 3.0759(5) nm^3, monoclinic, space group $P2_1/c$, Z = 8, D_x = 1.11 g cm^{-3}, μ = 13.24 cm^{-1}, and F(000) = 1 072.

Data collection. Scan speeds 1.5 – 8.0° min^{-1}, scan widths 1.05° + α-doublet splitting, 4.0° < 2θ < 50.0°, T = 200 K.

Structure refinement. Number of data collected 4 150, number observed [$F > 4.0\,\sigma(F)$] = 3 281, $R(R_w)$ = 0.0445(0.0510), number of parameters 372.

The authors thank the Royal Society, the SERC for a studentship (to J. H. J.), the Grant Agency of the Academy of Sciences of the Czech Republic (Grant No. 43204) and Borax Research Limited for support, Dr T. S. Griffin and Dr D. M. Wagnerová for their helpful cooperation, and Dr X. L. R. Fontaine and Dr D. Reed for NMR spectroscopy in the initial stages of this work. We thank Prof. N. N. Greenwood for his interest.

REFERENCES

1. Grimes R. N. in: *Comprehensive Organometallic Chemistry*, Part I (G. Wilkinson, F. G. A. Stone and E. Abel, Eds), Chap. 5.5, p. 459, and references cited therein. Pergamon, 1982.
2. Kennedy J. D.: Prog. Inorg. Chem. *32*, 519 (1984); *34*, 211 (1986).
3. Kukina G. A., Sergienko V. S., Porai-Koshits M. A., Baše K., Zakharova I. A.: Izv. Akad. Nauk SSSR, Ser. Khim. *1981*, 2838; Jones J. H., Baše K., Thornton-Pett M., Štíbr B., Kennedy J. D.: Unpublished results.
4. Beckett M. A., Crook J. E., Greenwood N. N., Kennedy J. D.: J. Chem. Soc., Dalton Trans. *1986*, 1879.
5. Cheek Y. M., Thornton-Pett M., Kennedy J. D.: Inorg. Chim. Acta *99*, L43 (1985).
6. Jones J. H., Fontaine X. L. R., Greenwood N. N., Kennedy J. D., Thornton-Pett M., Štíbr B., Langhoff H.: J. Organomet. Chem., *445*, C15 (1993).
7. Kennedy J. D., Štíbr B., Thornton-Pett M., Jelínek T.: Inorg. Chem. *30*, 4481 (1991); Kennedy J. D., Štíbr B., Jelínek T., Fontaine X. L. R., Thornton-Pett M.: Collect. Czech. Chem. Commun. *58*, 2090 (1993).

8. Štíbr B., Jelínek T., Kennedy J. D., Fontaine X. L. R., Thornton-Pett M.: J. Chem. Soc., Dalton Trans. *1993*, 1261.
9. Nestor K., Kennedy J. D., Štíbr B., Thornton-Pett M.: Collect. Czech. Chem. Commun. *57*, 1262 (1992).
10. Williams R. E.: Inorg. Chem. *10*, 210 (1971); Adv. Inorg. Chem. Radiochem. *18*, 64 (1976).
11. Wade K.: J. Chem. Soc., Chem. Commun. *1971*, 792; Adv. Inorg. Chem. Radiochem. *18*, 1 (1976).
12. Dobrott R. D., Lipscomb W. N.: J. Chem. Phys. *37*, 1779 (1962).
13. Bould J., Kennedy J. D., Thornton-Pett M.: J. Chem. Soc., Dalton Trans. *1992*, 563.
14. Bould J., Brint P., Kennedy J. D., Thornton-Pett M.: Acta Crystallogr., C *46*, 1010 (1990).
15. Rogozinski J.: *M.S. Thesis.* University of Leeds, Leeds 1984.
16. Kennedy J. D., MacInnes Y. M., Thornton-Pett M.: Unpublished results.
17. Heřmánek S., Hnyk D., Havlas Z.: J. Chem. Soc., Chem. Commun. *1989*, 1959.
18. Heřmánek S., Jelínek T., Plešek J., Štíbr B., Fusek J., Mareš F. in: *Proceedings of the Sixth International Meeting on Boron Chemistry, Bechyně 1987* (S. Heřmánek, Ed.), pp. 26 – 73. World Scientific Publishing Co. PTE, Singapore 1987.
19. Heřmánek S.: Chem. Rev. *92*, 325 (1992).
20. Bown M., Plešek J., Baše K., Štíbr B., Fontaine X. L. R., Greenwood N. N., Kennedy J. D.: Magn. Reson. Chem. *27*, 947 (1989).
21. Fontaine X. L. R., Kennedy J. D., McGrath M., Spalding T. R.: Magn. Reson. Chem. *29*, 711 (1991).
22. McFarlane W.: Proc. R. Soc. London *306*, 185 (1968).
23. Sheldrick G. M.: *SHELXS86, Program System for X-Ray Structure Solution.* University of Gottingen, Gottingen 1986.
24. Sheldrick G. M.: *SHELX76, Program System for X-Ray Structure Determination.* University of Cambridge, Cambridge 1976.

Translated by the author (B. Š.).